International Journal of Pharmaceutics 359 (2008) 25–34

Contents lists available at ScienceDirect

International Journal of Pharmaceutics

journal homepage: www.elsevier.com/locate/ijpharm

Air-coupled non-contact mechanical property determination of drug tablets

Ilgaz Akseli, Cetin Cetinkaya*

Department of Mechanical and Aeronautical Engineering, Center for Advanced Materials Processing, Wallace H. Coulter School of Engineering, Clarkson University, Potsdam, NY 13699-5725, USA

ARTICLE INFO

Article history:
Received 5 February 2008
Received in revised form 12 March 2008
Accepted 14 March 2008
Available online 22 March 2008

Keywords:
Drug tablet mechanical properties
Drug tablet characterization
Non-contact process pharmaceutical monitoring
Acoustic process monitoring
Process Analytical Technology

ABSTRACT

A non-contact/non-destructive technique for determining the mechanical properties of coated drug tablets is presented. In the current measurement approach, air-coupled excitation and laser interferometric detection are utilized and their effectiveness in characterizing the mechanical properties of a drug tablet by examining its vibrational resonance frequencies is demonstrated. The drug tablet is vibrated via an acoustic field of an air-coupled transducer in a frequency range sufficiently high to excite its several vibrational modes (harmonics). The tablet surface vibrational responses at measurement points are acquired by a laser vibrometer in a non-contact manner. An iterative computational procedure based on the finite element method is developed to extract the mechanical properties of the coated tablet from a subset of its measured resonance frequencies. The mechanical properties measured by this technique are compared to those obtained by a standard contact ultrasonic measurement method and a good agreement is found. Sensitivities of the resonance frequencies to the changes in the tablet mechanical properties are also obtained and discussed. The presented non-destructive technique requires no physical contact with the tablet and operates in the microsecond time-scale. Therefore, it could be employed for rapid monitoring and characterization applications.

1. Introduction

Physical (mechanical) properties and mechanical defects (e.g. cracks, capping, and delamination) of drug tablets may affect their therapeutic functions (Cetinkaya et al., 2006; Varghese and Cetinkaya, 2007). Most transient and residual stresses in a tablet are created during processing, handling, packing, and shipping of tablets. Such stresses can lead to material failures such as: capping, chipping, abrasion or even breakage of the tablets (Cetinkaya et al., 2006). In the current study, a non-contact/non-destructive technique for determining the mechanical properties of coated tablets, such as Young's moduli, Poisson's ratios and mass densities of the core and the coat using an air-coupled approach, is presented. Due to the elevated regulatory requirements and competitive market pressures, the demands to measure and evaluate the mechanical properties of drug tablets for controlling product quality in manufacturing have been increasing in the pharmaceutical industry. For example, for comprehensive quality assurance monitoring in the pharmaceutical industry the U.S. Food and Drug Administration (FDA) has initiated a guidance program entitled the Process Analytical Technology (PAT), which is often defined as a system for designing, analyzing, and controlling manufacturing through timely measurements (i.e. during processing) of critical quality and performance attributes of raw and in-process materials, and processes with the goal of ensuring final pharmaceutical product quality (Hussain et al., 2004). The characterization approach detailed in this study is targeted for such monitoring and evaluation tasks.

Mechanical properties of drug tablets (e.g. mechanical strength and hardness) are typically measured by destructive tests, such as breaking strength, axial tensile strength, bending and diametrical compression tests. Fell and Newton (1968) investigated the tensile strength of the tablets by diametrical compression tests. Micro-hardness measurements, such as Vickers and Brinell as well as Knoop tests, are currently employed for measuring the hardness of the core and the coat layers of the tablets (Berkovich, 1951; Jetzer et al., 1983). These destructive tests do not only damage the structure of the tablet and cause loss of product, but also provide limited information about the mechanical state of the core and coating layer of the tablet. An overall mechanical property of a tablet can also not accurately be assessed by a single-point measurement.

In the recent past, deformation and compaction characteristics of the tabletting materials have been intensely studied (Roberts and Rowe, 1987; Bassam et al., 1990; Payne et al., 1996; Roberts et al., 2000; Hancock et al., 2003). One common objective of these studies is to determine the powder behavior during compaction and

* Corresponding author. Tel.: +1 315 268 6514; fax: +1 315 268 6438.
E-mail address: cetin@clarkson.edu (C. Cetinkaya).

0378-5173/$ – see front matter © 2008 Elsevier B.V. All rights reserved.
doi:10.1016/j.ijpharm.2008.03.020

to understand the effect of processing and tabletting stages on the compaction properties of final products. Even though mechanical (physical) properties of tablets are known to potentially influence the tablet chemical and physical stability (due to mechanical defect generation over time), the accuracy of dosage (due to density distribution and defects) and the shelf life (due to residual stresses and defects), relatively few studies (Fell and Newton, 1968; Rigdway and Aulton, 1970; Stanley et al., 1981; Felton et al., 1996; Roberts and Rowe, 1999; Podczeck et al., 2006) have focused on the measurement of the actual mechanical properties of the tablet materials (e.g. the Young's modulus, tensile strength and Poisson's ratio of the core and coating layer). Felton et al. (1996) studied the mechanical properties of film-coated tablets including their tensile strength, Young's moduli and tensile toughness levels using a diametrical compression test.

The properties of coats play an important role in the stability and release performance of film-coated dosage forms (Akseli and Cetinkaya, 2008). Tablet coating has been effectively used to protect the stomach from being exposed to high concentrations of active ingredients, to provide a barrier to unpleasant taste or odor and to extend shelf life by protecting the ingredients from degradation by moisture and oxygen. Additionally, it is known that tablet coating improve the mechanical strength of the dosage form, preserving tablet integrity during packaging and shipping.

Linking powder properties to the mechanical properties of compacts has been a long-term objective in the pharmaceuticals industry due to its practical importance in the compaction process design. Payne et al. (1996) and Roberts et al. (2000) developed a molecular dynamics modeling approach for predicting the Young's moduli of compacts and tabletting materials from the properties of powder. A mechanical model of crystal structure was used to determine the crystal lattice energy, from which Young's moduli of a series of compacts prepared from aspirin and polymorphs of primidone, carbamazepine and sulphathiazole could be extracted. However, reportedly it is difficult to obtain the bulk elastic properties of tablet materials from the first-principle based molecular dynamics simulations.

It should be noted that, in order to predict physical (e.g. tablet mechanical strength and porosity) and chemical (e.g. content uniformity) properties of drug tablets, various non-destructive and non-contact indirect techniques are also used in various industrial applications, such as acoustic emission (AE) (Waring et al., 1987; Wong et al., 1991; Hakanen and Laine, 1993, 1995; Serris et al., 2002), spectroscopy-based approaches (IR (infrared), near-IR (NIR) (Morisseau and Rhodes, 1997; Kirsch and Drennen, 1999; Chen et al., 2001; Donoso et al., 2003; Blanco and Alcala, 2006; Otsuka and Yamane, 2006) As a laboratory technique, the X-ray microtomography method, based on the attenuation properties of X-ray in a material due its mass density and atomic number, is also utilized to determine material density, density distribution, powder packing and particle movement during compaction (Inman et al., 2007). Among these techniques, AE and NIR are well-established methods in the pharmaceutical industry. In AE, an acoustic sensor passively "listens" to sound waves generated by stresses within a material body during processing. Techniques based on AE are mainly used in the pharmaceutical industry to monitor process end-points and flow of granular materials and to predict the particle sizes and properties of the final granules and brittleness of tabletting materials. In addition, compaction monitoring has been an important application of AE. Wong et al. (1991) reported that it is possible to differentiate the deformation mechanisms of single crystals of lactose monohydrate and anhydrous lactose during compaction by AE. Wong et al. (1991) also reports that AE techniques can be employed to predict the compaction properties and brittleness of tabletting materials if the bulk material is characterized by a single crystal. Waring et al. (1987) and Hakanen and Laine (1993, 1995) investigated the AE of lactose, sodium chloride, microcrystalline cellulose and paracetamol during compression using an acoustic transducer coupled to a portable activity meter. Computationally analyzing the acoustic peaks related with the particle compression and decompression, it is concluded that the deformation mechanism and capping tendency can be predicted. Measuring AE from process chambers is also used for the identification of various phenomena that can occur during powder compaction of pharmaceutical products, such as granular rearrangement, fragmentation, visco-plastic deformation of grains or granules (Serris et al., 2002). AE is a passive acoustic technique, its applicability is somewhat restricted due to limited spectral properties of excitation mechanisms, and difficulties associated with deconvoluting acoustic signals emitted by powders and compacts from various noise sources and mechanisms.

As reviewed in Hardy and Cook (2003), techniques based on NIR are primarily used for monitoring and predicting the end-points of granulation and drying operations to determine faults in manufacturing processes (Blanco and Alcala, 2006; Otsuka and Yamane, 2006). Various NIR-based techniques are also utilized to predict tablet mechanical strength indirectly from the porosity of the tablet material. In general, an increase in tablet porosity due to compaction leads to a reduction in tablet strength and Young's modulus. The NIR approach relies on the observation that a decrease in tablet porosity results in an increase in NIR absorbance (Morisseau and Rhodes, 1997; Kirsch and Drennen, 1999; Chen et al., 2001; Donoso et al., 2003; Blanco and Alcala, 2006; Otsuka and Yamane, 2006). However, note that NIR is an indirect approach for the evaluation of the mechanical properties of pharmaceutical materials since it is based on the relationship between material porosity and tablet mechanical properties. In addition, its sensitive calibration and validation requirements for tablet hardness models remain a challenge since it is known that a slight variation in spectral peaks could invalidate a model.

2. Materials and methods

2.1. Materials

In the reported study, sample tablets (referred to as P-tablets in the current study) with an average mass of 200 mg and with the characteristic dimensions of 5.79 mm width, 11.45 mm length, 3.33 mm thickness and a coating thickness of 102.3 μm are used in the experiments. The tablet geometry is depicted in Fig. 1.

2.2. Experimental set-up and configurations

The experimental set-up developed for the current study incorporates a square pulser/receiver (Panametrics 5077PR), an air-coupled transducer (QMI AS120Ti), a laser vibrometer (Polytec OFV511), a vibrometer controller (Polytec OFV3001) and a digitizing oscilloscope (Tektronix TDS3052), as well as a vacuum handling apparatus consisting of a vacuum wand and a vacuum pump with a suction power of −30 kPa (FVW-110 Duovac). The instrumentation diagram of the experimental set-up utilized for non-contact mechanical property determination of drug tablets and a close-up image of the tablet during testing is depicted in Figs. 2 and 3. A square electrical pulse from the pulser/receiver unit excites the air-coupled transducer in its bandwidth. The acoustic field generated on the active surface of the transducer interacts with the tablet and its vibrational modes (harmonics) are excited. The laser vibrometer measures the transient out-of-plane motion of a particular point on the top surface of the vibrating tablet over a bandwidth of

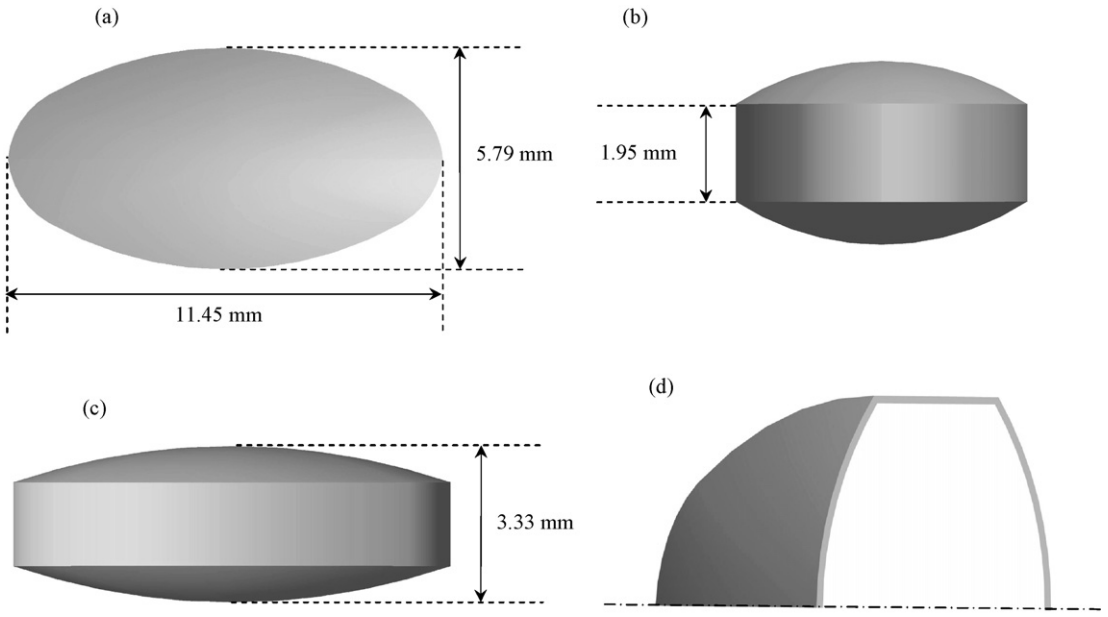

Fig. 1. The dimensions of a coated P-tablet with its top (a), front (b) and side (c) views. The coating thickness is 102.3 μm (d).

20 kHz to 30 MHz, with a sub-nanometer resolution in the range of ±75 nm. The diameter of the interferometric laser beam can be focused down to a few micrometers, so high resolution spatial scans are possible. Preliminary tests with various tablet fixing mechanisms indicate that the boundary conditions due to mounting techniques of a tablet can play an important role in the accuracy and sensitivity of transient response measurements. An ideal tablet holding configuration must not interfere with the acoustic field exciting the vibrational motion of the tablet, while holding the tablet firmly in place with a minimal contact area. In other words, weak elastic coupling between the tablet and the fixing mechanism is required. In the current study, a vacuum wand is utilized for holding the tablet. In the experiments conducted with the vacuum wand, a servo-motor controlled vacuum control unit is employed to automatically control suction power. The vacuum wand is also used to transport individual tablets from the tablet holding area

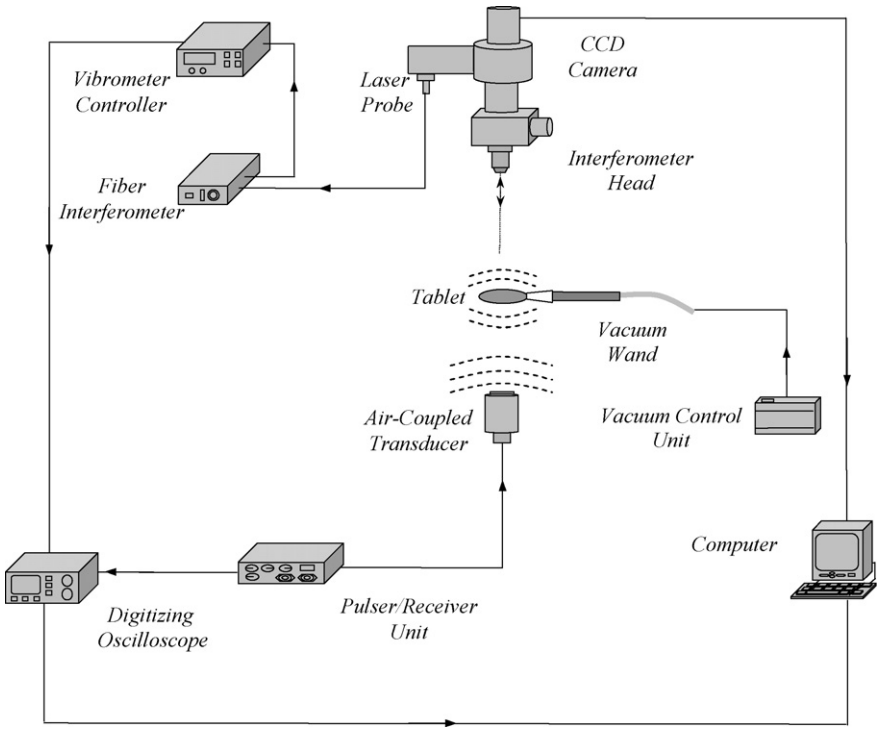

Fig. 2. Schematic of the instrumentation diagram of the experimental set-up for acquiring the out-of-plane motion of tablets.

Fig. 3. Image of the bottom excitation configuration using 120 kHz transducer with a vacuum wand holding the P-tablet in place. The vibrometer laser beam is visible on the top of the P-tablets.

to the test point (Fig. 3). The response of the vacuum wand to the air-coupled acoustic field was measured at several points on the wand, and no vibration of the wand with significant amplitudes was observed.

2.3. Experimental procedure for determining resonance frequencies

The frequency range of the measurements is limited to 105–150 kHz due to the bandwidth of the transducer employed in the experiments (Fig. 4). Since the bandwidth of the transducer overlaps with some of the resonance frequencies of the tablet, the propagating acoustic field generated by the transducer excites a number of its vibrational modes (harmonics). The tablet surface transient responses of a P-tablet at a number of measurement points are acquired by the vibrometer in a non-contact manner. The acquired waveforms (Fig. 5a–c) are digitized in the oscilloscope and uploaded to a computer for a spectral analysis to determine the vibrational resonance frequencies of the tablet (Fig. 5d). Consistent waveforms obtained at various points of P-tablets over an extended period of time indicate that the air-coupled excitation and the experimental set-up are repeatable. The mechanical property variations observed over time for the same tablets were less than 0.5%. A series of 50 P-tablets are employed for this work, but only the responses of three tablets are included for clarity. The resonance frequencies of all 50 tablets were consistent. In the vacuum wand mounting apparatus, the air-coupled transducer is placed under the sample P-tablet at the focal distance of the transducer in order to maximize the tablet–acoustic field interactions, and, consequently, the vibration amplitudes of the tablet motion (Fig. 3). The focal distance of the transducer is specified as approximately 2.35 mm. The laser vibrometer embedded into the optical microscope is focused at a point on the tablet surface through the objective lens of the microscope. The use of the micro-

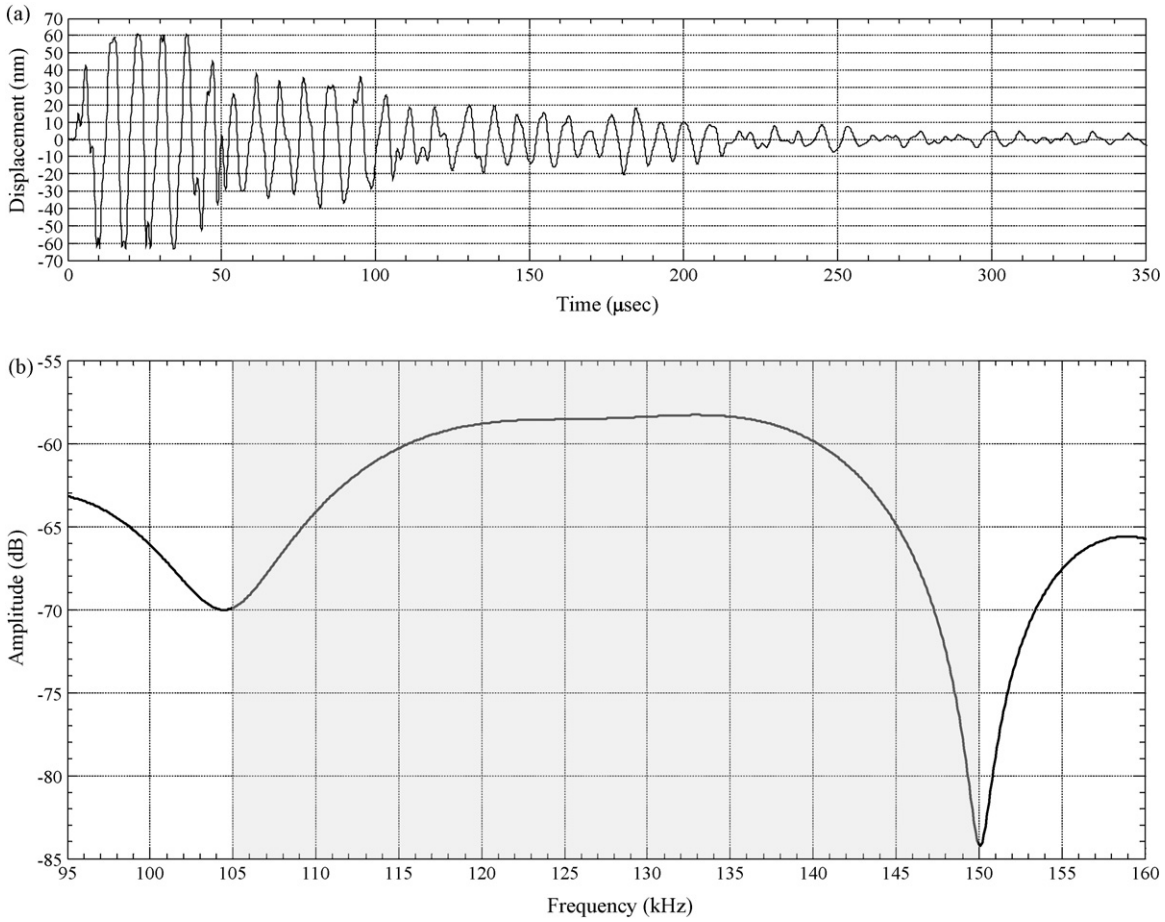

Fig. 4. Transient displacement (a) and frequency response (b) of a spot on the active surface of the 120 kHz transducer under a square pulse excitation with the pulse width of 8.33 μs and the amplitude of 100 V. Shaded area indicates the bandwidth of the air-coupled transducer.

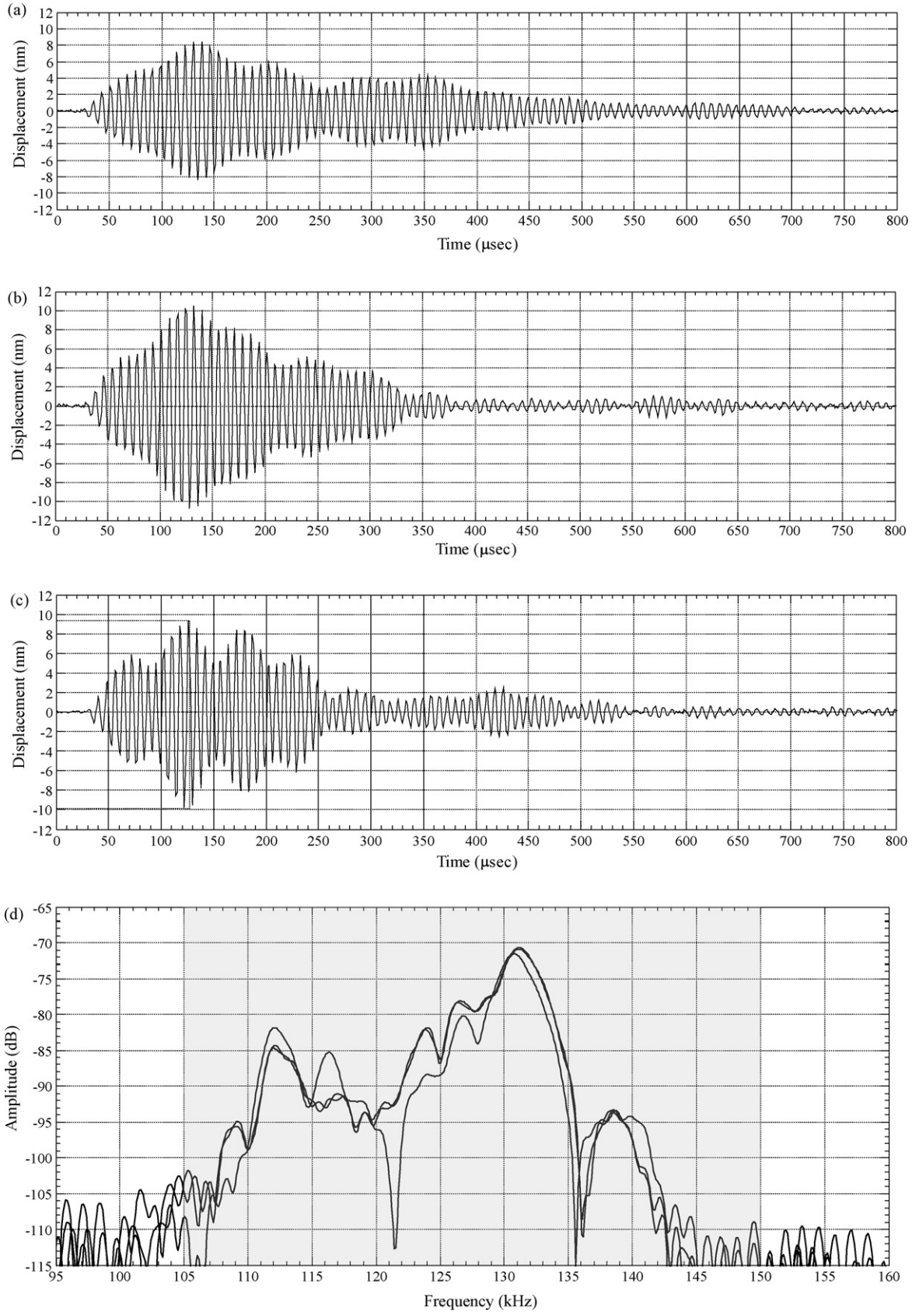

Fig. 5. Waveforms of three P-tablets held with the vacuum wand (a–c) and comparison of their frequency responses (d). Shaded area indicates the bandwidth of the air-coupled transducer.

Table 1
Summary of the numerical iteration results for the P-tablets

Mechanical properties	$\bar{p}*$	$\bar{p}_1^e$	$\bar{p}_2^e$	$\bar{p}_3^e$	$\bar{p}^c$	Convergence (%): $\bar{p}* - \bar{p}_i^e$		
						Tablet 1	Tablet 2	Tablet 3
E_{core} (MPa)	314.704	2648.220	2691.112	2666.287	2628.920†	19.125	17.227	18.318
ρ_{core} (kg/m^3)	1591.548	1335.763	1348.758	1329.848	1326.290†	19.207	18.001	19.679
ν_{core}	0.388	0.330	0.331	0.330	0.330*	17.575	17.185	17.576
E_{coat} (MPa)	3600.000	3023.150	3041.635	3038.521	3000*	19.081	18.357	18.478
ρ_{coat} (kg/m^3)	868.410	730.730	737.883	729.761	723.675†	18.841	17.689	18.999
ν_{coat}	0.447	0.382	0.385	0.381	0.380*	17.015	16.104	17.292

$\bar{p}*$ is the vector of starting mechanical property for the iterative computational procedure. $\bar{p}_1^e$, $\bar{p}_2^e$, $\bar{p}_3^e$ are the extracted mechanical property vectors upon completion of iterative procedure for $\bar{p}*$ for P-tablet 1, P-tablet 2, P-tablet 3, respectively. $\bar{p}^c$ is the measured and estimated mechanical property vector; E_{core} is calculated from the contact measurements, ρ_{core} and ρ_{coat} are calculated from direct mass measurements (†). Percentage convergences of initial and experimental mechanical property vectors are shown for three P-tablets. The estimated mechanical properties (ν_{core}, E_{coat}, ν_{coat}) for $\bar{p}^c$ are indicated by an asterix.

scope objective allows the laser probe beam to be focused at a spot that can be theoretically reduced to 0.5 (m using the 100× microscope objective. The P-tablet is placed under the objective at a distance of approximately 6.5 mm. The pulser/receiver unit used in this study can deliver up to a 400 V square pulse to the transmitting air-coupled transducer and provides a synchronizing pulse to trigger the digital oscilloscope. In the reported experiments, the pulser/receiver voltage was set to 100 V. As detailed below, using an iterative computational procedure, the mechanical properties of the P-tablet core and coating layer are extracted from a subset of the measured resonance frequencies in a specified bandwidth.

2.4. Contact measurements

For verification purposes, the Young's modulus of a P-tablet core (E_{core}) is obtained by utilizing a contact time-of-flight ultrasonic technique. The mass densities of the core (ρ_{core}) and the coating material (ρ_{coat}) of the P-tablet are calculated from direct mass measurements of tablets with various known coating thicknesses. Property predictions based on contact measurements are used for confirming the mechanical properties obtained by the air-coupled set-up. In determining the Young's modulus of the core material (E_{core}) of the P-tablet, a contact ultrasonic set-up operating in the pulse-echo mode is employed. In this test, a piezoelectric transducer (Aerotech Inc.) generates short ultrasonic pulses with a central frequency of 5 MHz to transmit through the tablet. The ultrasonic wavefront is reflected from the back side of the tablet and returned to the measurement surface via the shortest possible path. The reflected waveforms are captured by the same transducer and digitized in the oscilloscope. The thickness of the tablet is measured. The time-of-flight of an acoustic pulse is a function of the tablet thickness and the longitudinal velocity of sound c_L in the core material. Since the longitudinal velocity $c_L = \sqrt{E/\rho}$, the Young's modulus of the core can be extracted if the mass density of the core material is available. Consistent waveforms providing the

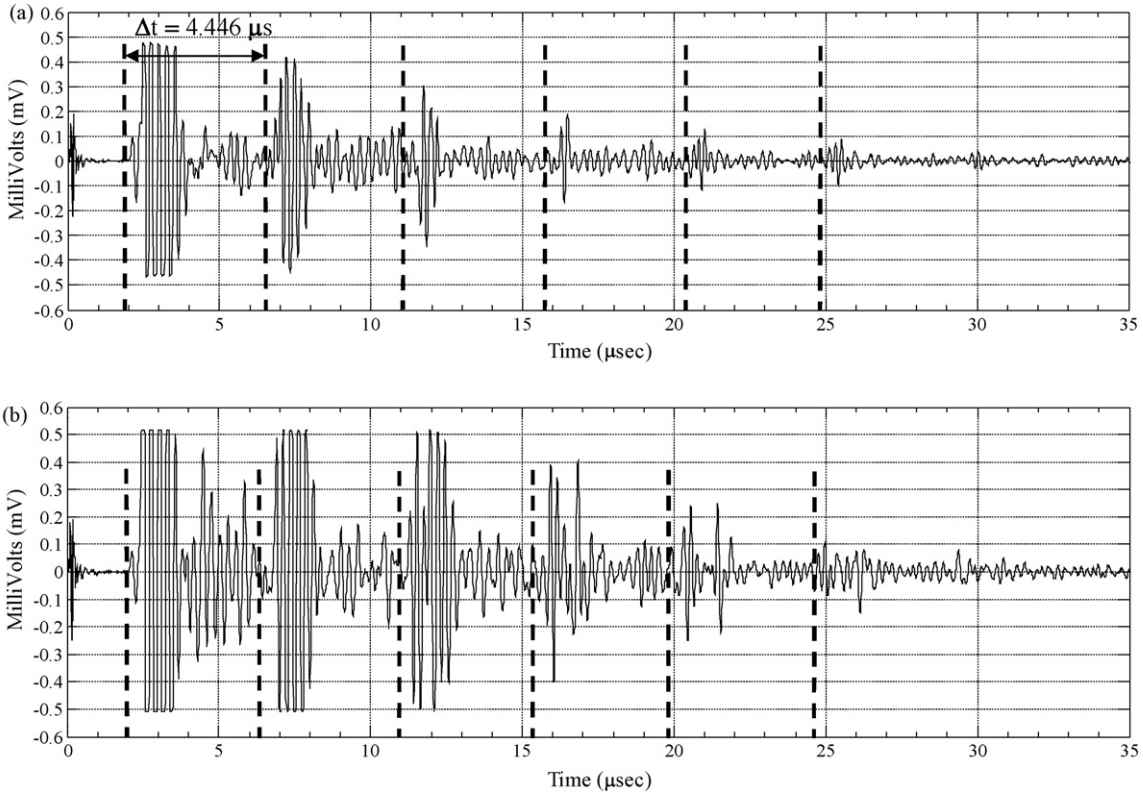

Fig. 6. Waveforms indicating the time-of-flight and multiple reflections across the tablet cross-section for two different P-tablets (a and b) in the pulse-echo mode. The first multiple reflection is used to determine time-of-flight through the tablet.

Table 2
Summary of the resonance frequencies for the P-tablets

Modes	$\bar{f}*$	$\bar{f}_1^e$	$\bar{f}_2^e$	$\bar{f}_3^e$	Convergence (%): $\bar{f}^* - \bar{f}_i^e$		
					Tablet 1	Tablet 2	Tablet 3
8	107,331	109,135	109,338	109,675	−1.653	−1.835	−2.137
9	112,089	112,175	113,391	113,750	−0.076	−1.148	−1.460
11	120,891	122,621	122,869	123,235	−1.411	−1.609	−1.902
13	122,150	123,863	124,118	124,492	−1.383	−1.585	−1.881
14	131,641	131,646	133,017	133,362	−0.004	−1.034	−1.290
15	136,547	138,418	138,776	138,157	−1.352	−1.606	−1.165
Modes	$\bar{f}^c$	$\bar{f}_{v_1}^e$	$\bar{f}_{v_2}^e$	$\bar{f}_{v_3}^e$	Error (%): $\bar{f}^c - \bar{f}_{v_i}^e$		
					Tablet 1	Tablet 2	Tablet 3
8	109,085	109,137	109,412	109,210	−0.047	−0.298	−0.114
9	112,149	112,181	111,910	112,150	−0.028	0.213	−0.00089
11	122,562	122,629	121,525	121,810	−0.054	0.853	0.617
13	123,821	123,870	123,805	124,115	−0.039	0.013	−0.237
14	131,627	131,655	131,220	131,830	−0.021	0.310	−0.154
15	137,425	138,480	138,505	138,155	−0.762	−0.779	−0.528

$\bar{f}*$ and $\bar{f}^c$ are the FE resonance frequency vectors corresponding to $\bar{p}*$ and $\bar{p}^c$, respectively. $\bar{f}_1^e$, $\bar{f}_2^e$, $\bar{f}_3^e$ are the FE resonance frequency vectors, upon completion of sensitivity analysis, corresponding to $\bar{p}_1^e$, $\bar{p}_2^e$, $\bar{p}_3^e$ of P-tablet 1, P-tablet 2, P-tablet 3, respectively. $\bar{f}_{v_1}^e$, $\bar{f}_{v_2}^e$, $\bar{f}_{v_3}^e$ are the experimental resonance frequency vectors directly measured with the vacuum wand for P-tablet 1, P-tablet 2, P-tablet 3, respectively.

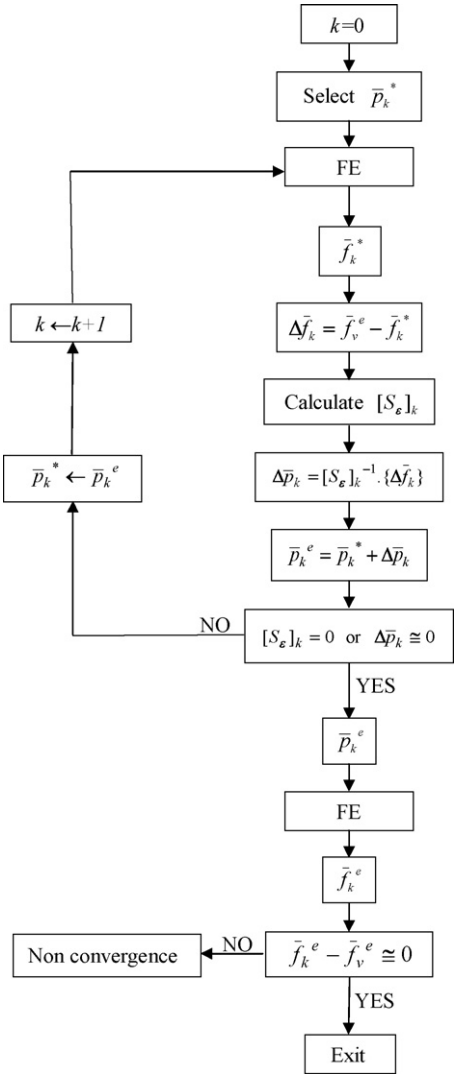

Fig. 7. Flow chart for the iterative process for extracting the mechanical properties of the core and the coat of a P-tablet.

time-of-flight across the tablet thickness for two different tablets are depicted in Fig. 6a and b. The computed Young's modulus of the core of the sample tablet (E_{core} = 2628.92 ± 3.5 MPa) is included in Table 1. The experimental error is due to 2% uncertainty in the time-of-flight measurements.

2.5. Finite element calculations for tablet spectral properties

Vibrational properties of a tablet are related to its mechanical properties (e.g. the Young's moduli (E_{core}, E_{coat}), Poisson's ratios (ν_{core}, ν_{coat}) and material mass densities (ρ_{core}, ρ_{coat}) of the core and the coating layer) as well as its geometry (e.g. the shape and dimensions of the core and the coating layer). Using a finite element (FE) algorithm, such as the Lanczos method, the spectral (harmonic) properties of the tablet (e.g. a set of resonance frequencies and corresponding mode shapes) can be obtained provided that the mechanical properties and geometry of the tablet are available. However, the extraction of the mechanical properties of a tablet from its measured resonance frequencies requires the use of an iterative computational procedure.

In the finite element study employed for computing the resonance frequencies of the tablets, the material of a three-

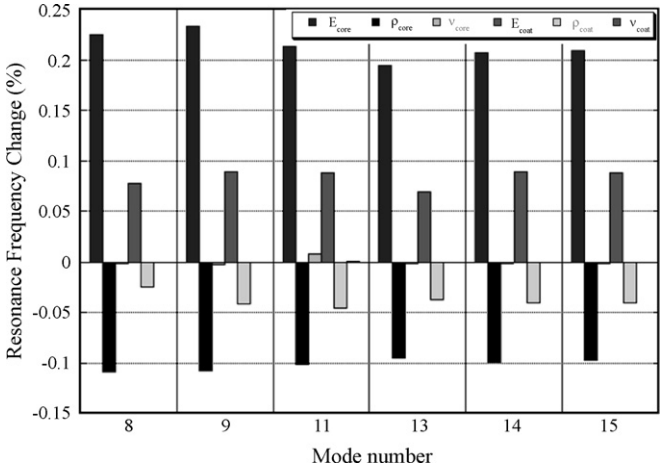

Fig. 8. Normalized sensitivities of the resonance frequencies of P-tablet 1 to the changes in E_{core}, ρ_{core}, ν_{core}, E_{coat}, ρ_{coat}, and ν_{coat} for the modes 8, 9, 11, 13, 14 and 15.

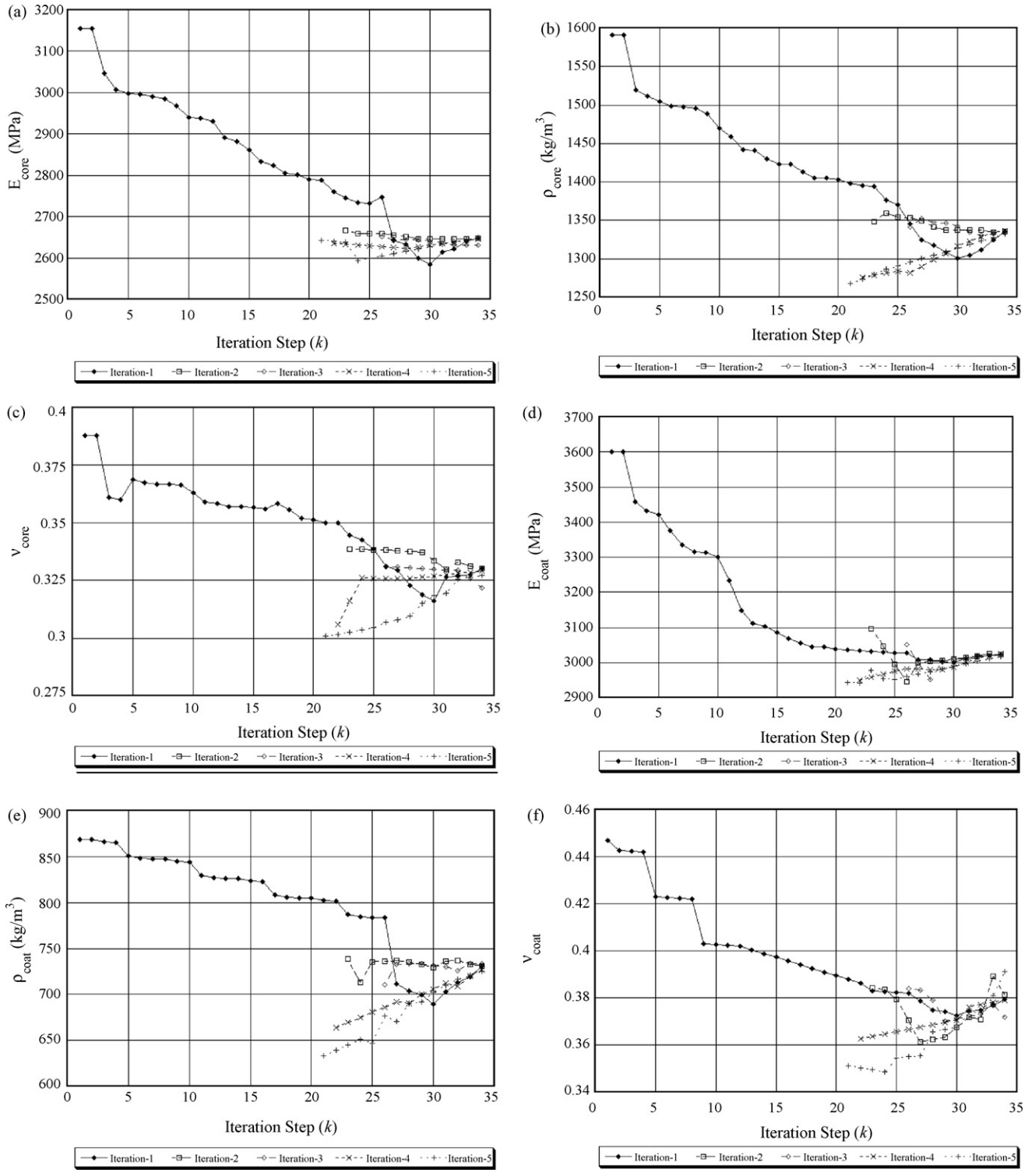

Fig. 9. Convergence of E_{core} (a), ρ_{core} (b), ν_{core} (c), E_{coat} (d), ρ_{coat} (e), and ν_{coat} (f) of the P-tablet 1 during the sensitivity iterations.

dimensional mesh for the tablet is modeled as homogenous and isotropic elastic solid consisting of a core and a coating layer. The top, front and side views illustrating outer dimensions and cross-sectional area of the coated P-tablet with a coating thickness of 102.3 μm used in the FE analysis are depicted in Fig. 1. Four-node linear tetrahedron elements are used in the mesh generation for the coated tablet. The number of elements, number of nodes, degrees of freedom and element size of the meshed coated tablet are 62,635, 14,357, 43,071, and 250 μm, respectively. The Lanczos eigenvalue solver implemented in the commercial software package ABAQUS (ABAQUS Theory Manual, 2007) is employed to obtain the resonance frequencies of the tablet in the frequency range of 40–200 kHz for given material properties.

2.6. Extracting tablet mechanical properties

In order to extract the mechanical property parameters (E_{core}, E_{coat}, ν_{core}, ν_{coat}, ρ_{core}, ρ_{coat}) of sample P-tablets from their measured resonance frequencies, an iterative procedure based on Newton's method is developed. From an FE study, it is observed that shifts in resonance frequencies are nearly linear with the relatively small changes in the mechanical properties, and no intersection of modes is realized within ±20% variation of the initial (estimate) mechanical properties. This large initial variation range is used to test the convergence effectiveness of the presented algorithm. If modes traverse as a result of the mechanical property variations, the corresponding resonance frequencies will not coincide with their ordered mode shapes, and all the mode shapes and corresponding resonance frequencies must be verified before continuing the extraction scheme. In this type of analysis for mechanical properties, a series of either numerical or actual tests are conducted in which the (mechanical) parameters are altered to approximate the relationships between changes in the (mechanical) parameters, and corresponding changes in the natural frequencies. The end result of such a study is a set of sensitivity coefficients that can be used to approximate the assumed relationship. From these sensitivity coefficients, the actual mechanical properties can approximately be extracted within the ranges of the parameters.

In the mechanical property extraction, a set of initial (estimated) mechanical property vector is chosen $\bar{p}_k^*$ (Table 1) and the corresponding resonance frequency vector $\bar{f}_k^*$ is calculated via the FE method for the given tablet geometry (Table 2) and each iteration step is denoted by index k. The reason for choosing a wide range for the initial (estimate) values is to demonstrate that the algorithm convergences even if the initial values are considerably off from their actual values. Each mechanical property parameter (E_{core}, ρ_{core}, ν_{core}, E_{coat}, ρ_{coat}, ν_{coat}) and vibrational mode numbers obtained from the FE are denoted by indices i and j, respectively. Consistent six modes calculated from the FE ($j = 1, 2, \ldots, 6$) for $\bar{p}_k^*$ are compared to the experimentally obtained resonance frequencies $\bar{f}_{v_1}^e, \bar{f}_{v_2}^e, \bar{f}_{v_3}^e$ (Table 2) for the three P-tablets selected for sensitivity calculations. The ith component of $\bar{p}_k^*$ is perturbed by a factor of $(1+\varepsilon)$ and the six resulting perturbed material property vectors are denoted by $\bar{p}_i$ ($i = 1, 2, \ldots, 6$). The FE model is run for each $\bar{p}_i$ to determine the corresponding six resonance frequency vectors $\bar{f}_i'$ and their shifts $\Delta\bar{f}_i = \bar{f}_i' - \bar{f}^*$. Using the first term in Taylor's expansion, the sensitivity coefficient vector $\{s\}$ is approximated for $i = 1, 2, \ldots, 6$ as:

$$\Delta\bar{f}_i \cong \{s\}^T \times \{\Delta p\} \tag{1}$$

where

$$\{\Delta p\} = \left\{ \Delta E_{core} \quad \Delta\rho_{core} \quad \Delta\upsilon_{core} \quad \Delta E_{coat} \quad \Delta\rho_{coat} \quad \Delta\nu_{coat} \right\}^T,$$

$$\{s\} = \left\{ \frac{\partial f_j}{\partial E_{core}} \quad \frac{\partial f_j}{\partial \rho_{core}} \quad \frac{\partial f_j}{\partial \nu_{core}} \quad \frac{\partial f_j}{\partial E_{coat}} \quad \frac{\partial f_j}{\partial \rho_{coat}} \quad \frac{\partial f_j}{\partial \nu_{coat}} \right\}^T,$$

j is the vibrational mode number, $\Delta p = \bar{p}_i - \bar{p}^*$, $\{s\}$ the sensitivity coefficient vector and $\Delta\bar{f}_i = \bar{f}_i' - \bar{f}^*$. After running the FE model and applying Eq. (1) for $i = 1, 2, \ldots, 6$ to calculate the sensitivity coefficients for six modes $j = 1, 2, \ldots, 6$ (not necessarily sequential), the sensitivity tangent matrix $[S_\varepsilon]_k$ is constructed for the six modes:

$$[S_\varepsilon]_k = \begin{bmatrix} \frac{\partial f_1}{\partial E_{core}} & \frac{\partial f_1}{\partial \rho_{core}} & \frac{\partial f_1}{\partial \nu_{core}} & \frac{\partial f_1}{\partial E_{coat}} & \frac{\partial f_1}{\partial \rho_{coat}} & \frac{\partial f_1}{\partial \nu_{coat}} \\ \frac{\partial f_2}{\partial E_{core}} & \frac{\partial f_2}{\partial \rho_{core}} & \frac{\partial f_2}{\partial \nu_{core}} & \frac{\partial f_2}{\partial E_{coat}} & \frac{\partial f_2}{\partial \rho_{coat}} & \frac{\partial f_2}{\partial \nu_{coat}} \\ \frac{\partial f_3}{\partial E_{core}} & \frac{\partial f_3}{\partial \rho_{core}} & \frac{\partial f_3}{\partial \nu_{core}} & \frac{\partial f_3}{\partial E_{coat}} & \frac{\partial f_3}{\partial \rho_{coat}} & \frac{\partial f_3}{\partial \nu_{coat}} \\ \frac{\partial f_4}{\partial E_{core}} & \frac{\partial f_4}{\partial \rho_{core}} & \frac{\partial f_4}{\partial \nu_{core}} & \frac{\partial f_4}{\partial E_{coat}} & \frac{\partial f_4}{\partial \rho_{coat}} & \frac{\partial f_4}{\partial \nu_{coat}} \\ \frac{\partial f_5}{\partial E_{core}} & \frac{\partial f_5}{\partial \rho_{core}} & \frac{\partial f_5}{\partial \nu_{core}} & \frac{\partial f_5}{\partial E_{coat}} & \frac{\partial f_5}{\partial \rho_{coat}} & \frac{\partial f_5}{\partial \nu_{coat}} \\ \frac{\partial f_6}{\partial E_{core}} & \frac{\partial f_6}{\partial \rho_{core}} & \frac{\partial f_6}{\partial \nu_{core}} & \frac{\partial f_6}{\partial E_{coat}} & \frac{\partial f_6}{\partial \rho_{coat}} & \frac{\partial f_6}{\partial \nu_{coat}} \end{bmatrix} \tag{2}$$

Using $[S_\varepsilon]_k$, the change in mechanical properties vector due to a shift $\{\Delta\bar{f}_k\}$ in the selected set of resonance frequencies can be approximated by

$$\{\Delta\bar{p}\}_k = [S_\varepsilon]_k^{-1} \times \{\Delta\bar{f}_k\} \tag{3}$$

where $\Delta\bar{f}_k = \bar{f}_v^e - \bar{f}_k^*$, and $\{\Delta\bar{p}\}_k$ the change in mechanical properties after the completion of an iteration with the perturbation $\bar{p}_k^e = \bar{p}_k * + \Delta\bar{p}_k$ (see Table 1 for their numerical values). In this study, a number of iterations are executed to approximate a set of values for E_{core}, E_{coat}, ν_{core}, ν_{coat}, ρ_{core} and ρ_{coat}. Once singularity is observed in the tangent matrix $[S_\varepsilon]_k$ or $\{\Delta\bar{p}\}_k$ values converge to zero, the iteration loop is terminated. The values of $\bar{p}^*$ used in the last iteration correspond to the experimental mechanical property vector $\bar{p}_k^e$ of the core and coating of the tablet since $\Delta\bar{p}_k \cong 0$ (see Table 1 for the numerical values for the three P-tablets). A flow chart for this iterative process is depicted in Fig. 7.

3. Results and discussion

To validate the extracted mechanical properties of the three P-tablets, the FE method is employed to determine the corresponding resonance frequency vectors $\bar{f}_1^e, \bar{f}_2^e, \bar{f}_3^e$, for comparison purposes (see Table 2 for their numerical values). Due to tablet-to-tablet variations, small differences are detected in the resonance frequencies and corresponding mechanical properties among three P-tablets. Within ±20% variations of the mechanical properties, changes in resonance frequencies are calculated approximately in the range of ±1.5% as listed in Tables 1 and 2. The percent error between the measured resonance frequencies ($\bar{f}_{v_1}^e, \bar{f}_{v_2}^e, \bar{f}_{v_3}^e$) and the calculated resonance frequencies ($\bar{f}_1^e, \bar{f}_2^e, \bar{f}_3^e$) corresponding to extracted mechanical properties is within ±1.5% for three sample tablets (Table 2). It is also determined that the sensitivity order of resonance frequencies regarding changes in the mechanical properties, in decreasing order, are; E_{core}, ρ_{core}, E_{coat}, ρ_{coat}, ν_{core} and ν_{coat} (Fig. 8). Convergence of the mechanical property parameters of Tablet 1 in the iterative loop is depicted in Fig. 9. In addition, local convergence of each mechanical property has been demonstrated in Fig. 9.

4. Conclusions and remarks

In the present study, a non-destructive/non-contact testing platform based on air-coupled acoustics for determining the mechanical properties of drug tablets is developed and described. A computational procedure for extracting mechanical property parameters from the measured resonance frequencies of tablets is developed and implemented. The effectiveness of the procedure for extracting the mechanical properties (Young's moduli, Poisson's ratios and mass densities) of a core and coating layer of a tablet from its experimentally obtained resonance frequencies is demonstrated. It is established that mechanical properties

can be extracted utilizing the proposed experimental methodology and the iterative computational procedure based on the measured resonance frequencies of the tablet. The acquired experimental resonance frequencies agree quantitatively well with the FE-based resonance frequencies corresponding to the extracted mechanical properties. In addition, a standard contact ultrasonic method was successfully employed to verify the air-coupled Young's modulus measurements. Analysis also revealed that the resonance frequencies of a sample tablet are most sensitive to changes in E_{core}, and least sensitive to changes in ν_{coat}. Note that this observation holds for the bandwidth of the air-coupled transducer (105–150 kHz) considered in current study. In this frequency range, it is easier to extract the Young's modulus of the core than the Poisson's ratio of the coat since the resonance frequencies are less sensitive to the Poisson's ratios of the materials. It is reasonable to anticipate that, using the FE method, one can identify a certain set of mode shapes and, thus, the frequency ranges (the bandwidth of the transducer) in which the locations of the resonance frequencies are more sensitive to the Poisson's ratios of the materials. Such knowledge can play a key role in monitoring and characterization applications since it could allow the user to identify the required bandwidth and, consequently, the specification of a transducer for a particular application.

The potential of air-coupled acoustics as a characterization method for determination of the tablet mechanical properties and coat thickness is demonstrated. The adoption of this technology as a general purpose pharmaceutical release test tool (such as a PAT tool) will, however, require further research and development work to satisfy method validation requirements.

Acknowledgements

The authors thank Dr. Dominic A. Ventura for stimulating discussions and acknowledge the Consortium for the Advancement of Manufacturing of Pharmaceuticals (CAMP) and the Center for Advanced Materials Processing (CAMP) at Clarkson University for their partial funding. The interferometric equipment used in this study was acquired through a grant from the National Science Foundation (Nanoscale Exploratory Research Program, Award ID 0210242).

References

ABAQUS Theory Manual, 2007. Version 6.7, Dassault Systèmes SIMULIA Corporation, pp. 2.4.1-1–2.4.1-7.

Akseli, I., Cetinkaya, C., 2008. Drug tablet thickness estimations using air-coupled acoustics. Int. J. Pharm. 351, 165–173.

Bassam, F., York, P., Rowe, R.C., Roberts, R.J., 1990. Young's modulus of powders used as pharmaceutical excipients. Int. J. Pharm. 64, 55–60.

Berkovich, E.S., 1951. Three-faceted diamond pyramid for micro-hardness testing. Ind. Diamond Rev. 11, 129–132.

Blanco, M., Alcala, M., 2006. Content uniformity and tablet hardness testing of intact pharmaceutical tablets by near infrared spectroscopy – a contribution to process analytical technologies. Anal. Chim. Acta 557, 353–359.

Cetinkaya, C., Akseli, I., Mani, G.N., Libordi, C.F., Varghese, I., 2006. Non-contact mechanical characterization and testing of drug tablets. In: Kundu, T. (Ed.), Advanced Ultrasonic Methods for Material and Structure Inspection. ISTE Science and Technical Publishing, UK, pp. 319–369.

Chen, Y.X., Thosar, S.S., Forbess, R.A., Kemper, M.S., Rubinovitz, R.L., Shukla, A.J., 2001. Prediction of drug content and hardness of intact tablets using artificial neural network and near-infrared spectroscopy. Drug Dev. Ind. Pharm. 27, 623–631.

Donoso, M., Kildsig, D.O., Ghaly, E.S., 2003. Prediction of tablet hardness and porosity using near-infrared diffuse reflectance spectroscopy as a nondestructive method. Pharm. Dev. Technol. 8, 357–366.

Fell, J.T., Newton, J.M., 1968. Tensile strength of lactose tablets. J. Pharm. Pharmacol. 20, 657–659.

Felton, L.A., Shah, N.H., Zhang, G., Infeld, M.H., Malick, A.W., McGinity, J.W., 1996. Physical–mechanical properties of film-coated soft gelatin capsules. Int. J. Pharm. 127, 203–211.

Hakanen, A., Laine, E., 1993. Acoustic emission during powder compaction and its frequency spectral analysis. Drug Dev. Ind. Pharm. 19, 2539–2560.

Hakanen, A., Laine, E., 1995. Acoustic characterization of a micro-crystalline cellulose powder during and after its compression. Drug Dev. Ind. Pharm. 21, 1573–1582.

Hancock, B.C., Colvin, J.T., Mullarney, M.P., Zinchuk, A.V., 2003. The relative densities of pharmaceutical powders, blends, dry granulations, and immediate-release tablets. Pharm. Technol. 27, 64–80.

Hardy, I.J., Cook, W.G., 2003. Predictive and correlative techniques for the design, optimization and manufacture of solid dosage forms. J. Pharm. Pharmacol. 55, 3–18.

Hussain, A.S., Watts, C., Afnan, A.M., Wu, H., 2004. Foreword. J. Process Anal. Technol. 1, 3–4.

Inman, S.J., Briscoe, B.J., Pitt, K.G., 2007. Topographic characterization of cellulose bilayered tablets interfaces. Chem. Eng. Res. Des. 85, 1005–1012.

Jetzer, W., Leuenberger, H., Sucker, H., 1983. The compressibility and compatibility of pharmaceutical powders. Pharm. Technol. 7, 33–39.

Kirsch, J.D., Drennen, J.K., 1999. Nondestructive tablet hardness testing by near-infrared spectroscopy: a new and robust spectral best-fit algorithm. J. Pharm. Biomed. Anal. 19, 351–362.

Morisseau, K.M., Rhodes, C.T., 1997. Near-infrared spectroscopy as a nondestructive alternative to conventional tablet hardness testing. Pharm. Res. 14, 108–111.

Otsuka, M., Yamane, I., 2006. Prediction of tablet hardness based on near infrared spectra of raw mixed powders by chemometrics. J. Pharm. Sci. 95, 1425–1433.

Payne, R.S., Roberts, R.J., Rowe, R.C., McPartlin, M., Bashall, A., 1996. The mechanical properties of two forms of primidone predicted from their crystal structures. Int. J. Pharm. 145, 165–173.

Podczeck, F., Drake, K.R., Newton, J.M., Haririan, I., 2006. The strength of bilayered tablet. Eur. J. Pharm. Sci. 29, 361–366.

Rigdway, K., Aulton, M.E., 1970. The surface hardness of tablets. J. Pharm. Pharmacol. 22, 70–78.

Roberts, R.J., Rowe, R.C., 1987. The Young's modulus of pharmaceutical materials. Int. J. Pharm. 37, 15–18.

Roberts, R.J., Rowe, R.C., 1999. Relationships between the modulus of elasticity and tensile strength for pharmaceutical drugs and excipients. J. Pharm. Pharmacol. 51, 975–977.

Roberts, R.J., Payne, R.S., Rowe, R.C., 2000. Mechanical property predictions for polymorphs of sulphathiazole and carbamazepine. Eur. J. Pharm. Sci. 9, 277–283.

Serris, E., Camby-Perier, L., Thomas, G., Desfontaines, M., Fantozzi, G., 2002. Acoustic emission of pharmaceutical powders during compaction. Powder Technol. 128, 296–299.

Stanley, P., Rowe, R.C., Newton, J.M., 1981. Theoretical considerations of the influence of polymer film coatings on the mechanical strength of tablets. J. Pharm. Pharmacol. 33, 557–560.

Varghese, I., Cetinkaya, C., 2007. Non-contact photo-acoustic defect detection in drug tablets. J. Pharm. Sci. 96, 2125–2133.

Waring, M.J., Rubinstein, M.H., Howard, J.R., 1987. Acoustic emission of pharmaceutical materials during compression. Int. J. Pharm. 36, 29–36.

Wong, D.Y.T., Waring, M.J., Wright, P., Aulton, M.E., 1991. Elucidation of the compressive deformation behavior of α-lactose monohydrate and anhydrous α-lactose single crystals by mechanical strength and acoustic emission analyses. Int. J. Pharm. 72, 233–241.